## Research Article

# The Identification of Core Gene Expression Signature in Hepatocellular Carcinoma

**Ning Li [iD],[1] Ling Li,[2] and Yongshun Chen [iD][3]**

[1]Department of Cardiology, Renmin Hospital of Wuhan University, Cardiovascular Research Institute, Wuhan University and Hubei Key Laboratory of Cardiology, Wuhan 430060, China
[2]Institute of Hepatobiliary Diseases of Wuhan University, Zhongnan Hospital of Wuhan University and Hubei Key Laboratory of Medical Technology on Transplantation, Wuhan, Hubei 430071, China
[3]Department of Clinical Oncology, Renmin Hospital of Wuhan University, Wuhan 430060, China

Correspondence should be addressed to Yongshun Chen; yongshun2007@163.com

Hepatocellular carcinoma (HCC) is one of the most common malignancies, which causes serious financial burden worldwide. This study aims to investigate the potential mechanisms contributing to HCC and identify core biomarkers. The HCC gene expression profile GSE41804 was picked out to analyze the differentially expressed genes (DEGs). Gene ontology (GO) and the Kyoto Encyclopedia of Genes and Genomes (KEGG) analyses were carried out using DAVID. We constructed a protein-protein interaction (PPI) network to visualize interactions of the DEGs. The survival analysis of these hub genes was conducted to evaluate their potential effects on HCC. In this analysis, 503 DEGs were captured (360 downregulated genes and 143 upregulated genes). Meanwhile, 15 hub genes were identified. GO analysis showed that the DEGs were mainly enriched in oxidative stress, cell cycle, and extracellular structure. KEGG analysis suggested the DEGs were enriched in the absorption, metabolism, and cell cycle pathway. PPI network disclosed that the top3 modules were mainly enriched in cell cycle, oxidative stress, and liver detoxification. In conclusion, our analysis uncovered that the alterations of oxidative stress and cell cycle are two major signatures of HCC. TOP2A, CCNB1, and KIF4A might promote the development of HCC, especially in proliferation and differentiation, which could be novel biomarkers and targets for diagnosis and treatment of HCC.

## 1. Introduction

Primary liver cancer, the sixth most common cancer overall, is causing the second largest number of cancer death all over the world. Hepatocellular carcinoma (HCC) is a predominant primary liver cancer, accounting for approximately 90% of all types of primary hepatic malignancy and triggering a major international public health problem [1]. The pathogenesis of HCC is a multistep process implicated with the progressive accumulation of gene alterations that pinpoint various cellular and molecular events including oxidative stress, endoplasmic reticulum stress, and abnormal cell cycle [2]. Take oxidative stress, for example, the increased production of reactive nitrogen species (RNS) or reactive oxygen species (ROS), in addition to the reduced antioxidant

defense, can accelerate the progression of HCC. To be more specific, oxidative stress damage affects the gene expression of cellular survival, the products of which can promote the proliferation and differentiation of normal cells and eventually lead to the reduction of cellular apoptosis or even the formation of the tumor cells [3].

A great body of studies have disclosed that the tumorigenesis and progression of HCC are implicated with the mutation and abnormal expression and of genes, involving epidermal growth factor receptor (EGFR) [4], cyclin D1 (CCND1) [5], FoxQ1 [6], c-myc [7], as well as mutations of some tumor-suppressor genes. However, in clinic, the serum detection of alpha-fetoprotein (AFP), magnetic resonance imaging (MRI), or dynamic computed tomography (CT) scan are the conventional methods for the diagnosis and

treatment of HCC. Lacking the specificity of auxiliary examination biomarker, it was thus difficult for physicians to achieve accurate diagnosis and treatment of HCC as early as possible, so some patients missed the optimal chance for surgery, thus increasing the risk of death [8]. Hence, the identification of specific and sensitive biomarkers which can assistant us to confirm patients at a lower or higher risk of death from HCC is of great significance, not only for more precise diagnosis, optimal treatment, and better prognosis, but also for a comprehensive understanding of the cellular and molecular mechanisms involved in carcinogenesis.

The recent adoption of high-throughput gene microarray in analyzing tumors and normal samples from patients and healthy individuals enables us to share and explore the global molecular landscapes of tumors at multiple levels ranging from somatic mutations and copy number alterations at the genome level to gene expression at transcriptome level, as well as epigenetic alterations [9–11]. However, the application of microarrays in clinic is limited to a great extent because of countless genes identified by gene profiling, lack of both independent validation and repeatability, as well as the complicated statistical analyses. To put these expression profiles in clinical practice as quickly as possible, it is necessary to identify a suitable amount of genes and develop a proper approach that could be operated by routine assay.

In this study, we downloaded GSE41804 from the Gene Expression Omnibus (GEO, http://www.ncbi.nlm.nih.gov/geo/) and utilized the GEO2R online tool to comprehensively identify the differentially expressed genes (DEGs). Whereafter, we established protein-protein interaction (PPI) network of the DEGs and selected the top 15 hub genes with a high degree of connectivity. Furthermore, we analyzed the gene ontology involving biological process (BP), molecular function (MF), cellular component (CC), and KEGG pathways of the DEGs. Additionally, we constructed three modules and verified their enriched pathways. Meanwhile, overall survival (OS) analysis of the top 15 hub genes were carried out based on the Gene Expression Profiling Interactive Analysis online database (http://gepia.cancer-pku.cn/). Finally, we chose 3 genes to further identify the correlation by comparing the level of the 3 genes and their protein expression in tumor and normal tissues based on The Human Protein Atlas database (http://www.proteinatlas.org).

## 2. Materials and Methods

*2.1. Microarray Data.* We downloaded the gene expression profile of GSE41804 from the GEO database, which was a free and publicly available database. The GSE41804 dataset has a total of 40 samples, containing 20 HCC samples and 20 normal liver tissues, which was based on agilent GPL570 platform ([HG-U133_Plus_2] Affymetrix Human Genome U133 Plus 2.0 Array) by Hodo et al. We also downloaded the Series Matrix File of GSE41804 from the GEO database.

*2.2. Screen Genes of Differential Expression.* The differentially expressed genes (DEGs) between HCC samples and normal liver samples were analyzed using GEO2R (https://www.ncbi.nlm.nih.gov/geo/geo2r/), an interactive online analysis

tool for the GEO database, which was based on R language. We defined DEGs as differentially expressed with $logFC < -2$ (upregulated genes) or $logFC > 2$ (downregulated genes), according to the criteria described in [12, 13]. The adjusted $P$ value $< 0.05$ was regarded statistically significant, which was used to decrease the false positive rate. Then, 503 DEGs were found, including 360 upregulated genes and 143 downregulated genes, and we selected the top 15 genes with a high degree of connectivity as hub genes.

In addition, we used visual hierarchical cluster analysis to show the heat map and volcano plot of two groups by ImageGP (http://www.ehbio.com/ImageGP/index.php/Home/Index/index.html) after the relative raw data of TXT files were downloaded.

*2.3. Gene Ontology and KEGG Pathway Analysis of DEGs.* Gene ontology (GO) analysis can annotate genes and their products with functions involving cellular components, molecular function, as well as biological pathways [14]. The Kyoto Encyclopedia of Genes and Genomes (KEGG) is a collection of databases that could handle genomes and biological pathways associated with diseases and drugs. KEGG essentially is a resource for the comprehensive understanding of biological systems and some high-level genome functional information [15]. The Database for Annotation, Visualization and Integrated Discovery (DAVID, http://david.ncifcrf.gov) (version 6.7) is an online biological information database which has integrated a bulk of biological data and corresponding analysis tools, thereby providing systematic and comprehensive biological function annotation information for high throughput gene expression [16]. $P < 0.05$ was regarded as the cut-off criterion with statistic difference. To visualize the key molecular functions, biological processes, cellular components, as well as pathways of DEGs, biological analyses were carried out by the DAVID online database.

*2.4. PPI Network and Module Analysis.* The Search Tool for the Retrieval of Interacting Genes (STRING) is an online tool that was designed to assess and integrate the protein-protein interaction (PPI) information, such as physical and functional associations. Up to now, a total of 9,643,763 proteins from 2031 organisms have been covered in STRING version 10.0 [17] To evaluate the interactional correlation of these DEGs, we first drew DEGs by STRING and then utilized the Cytoscape software to construct a PPI network. Meanwhile, we set a maximum number of interactors $= 0$ and a confidence score $\geq 0.4$ as the cut off criterion. Additionally, the Molecular Complex Detection (MCODE) app was also employed to select modules of the PPI network in the Cytoscape according to node score cut $-$ of f $= 0.2$, degree cut $-$ o f f $= 2$, max. depth $= 100$, and $k -$ core $= 2$. The pathway analysis of genes in the three modules was carried out based on DAVID, respectively. Also, 15 hub genes were mapped into STRING according to confidence score $\geq 0.4$ and maximum number of interactors $\leq 5$. We also used GO and KEGG pathway analysis to investigate their potential information.

*2.5. Comparison of the Hub Gene Expression Level.* GEPIA (http://gepia.cancer-pku.cn/index.html) is a newly developed

interactive web server designed by Zefang Tang, Chenwei Li, and Boxi Kang of Zhang Lab, Peking University, aimed at analyzing the RNA sequencing expression data of 9736 tumors and 8587 normal samples from the TCGA and the GTEx projects, using a standard processing pipeline. GEPIA provides customizable functions such as tumor/normal differential expression analysis, profiling according to cancer types or pathological stages, patient survival analysis, similar gene detection, correlation analysis, and dimensionality reduction analysis [18]. In our study, we mainly employed the boxplot to visualize the expression of hub genes in HCC and normal liver tissues. Then we selected two suspicious genes to analyze their correlation in a scatter diagram. The Human Protein Atlas (HPA, https://www.proteinatlas.org/) is a Swedish-based program initiated in 2003 with the aim to map all human proteins in cells, tissues, and organs using the integration of various omics technologies, including antibody-based imaging, mass spectrometry-based proteomics, transcriptomics, and systems biology [19]. By acquiring immunohistochemical data of patients with or without HCC based on HPA, we further verified the expression of these hub genes.

*2.6. Survival Analysis of Hub Genes.* The relapse-free and overall survival information were based on GEPIA database. The hazard ratio (HR) with 95% confidence intervals and logrank $P$ value were calculated and displayed on the plot. $P < 0.05$ was considered statistically significant.

*2.7. Gene Set Enrichment Analysis.* 20 HCC samples from GSE41804 were divided into two groups (high versus low) according to the expression level of CCNB2, and the median expression value was regarded as the cut-off point. In order to investigate the potential function of CCNB2, GSEA (http:// software.broadinstitute.org/gsea/index.jsp) was carried out between the two groups. Annotated gene sets c2.cp.kegg. v5.2.symbols.gmt, sets c2.cp.bp. v5.2.symbols.gmt, sets c2.cp.mf. v5.2.symbols.gmt, and sets c2.cp.cc. v5.2.symbols.gmt were selected as the reference gene sets. FDR $< 0.05$, |enrichment score $(ES)| > 0.5$ and gene size $\geq 100$ were regarded as the cut-off criteria.

*2.8. Reidentification of Oxidative Stress in HCC.* To further verify the vital role of oxidative stress in HCC, we detected the level of some typical markers in carcinoma tissue and adjacent tissue obtained from 6 patients with HCC. The level of superoxide dismutase (SOD), malondialdehyde (MDA), and glutathione peroxidase (GSH-Px) were determined using an assay kit (Beyotime, China) according to the standard operational process. Meanwhile, the mRNA level of NADPH P67 and gp91 were also measured in carcinoma tissue and adjacent tissue. Additionally, the protein expression of SOD, 4-hydroxynonenal (4-HNE), and p65 were also quantified using Western blot. Immunohistochemical staining further verified the expression of 4-HNE in carcinoma tissue and adjacent tissue. The study was carried out in accordance with legal requirements and supported by the Ethics Committee of Renmin Hospital of Wuhan University.

*2.9. Statistical Analysis.* All values are presented as the mean $\pm$ SD. All statistical analyses were performed by SPSS 19.0 software. A difference of $P < 0.05$ was considered statistically significant.

# 3. Results

*3.1. Identification of DEGs and Hub Genes.* There were 20 HCC samples and 20 normal samples in the study. The GEO2R online analysis tool was applied to detect the DEGs, using adjusted $P$ value $< 0.05$ and logFC $\geq 2$ or logFC $\leq -2$ as cut-off criteria. A total of 503 DEGs were captured after analyzing GSE41804, 360 of which were downregulated genes while 143 were upregulated (Figure 1(b)). The expression level of the top 50 DEGs with fold change 2 was displayed in (Figure 1(a)). Additionally, 15 hub genes were identified according to their degree of connectivity from high to low (Table1).

*3.2. GO Function and KEGG Pathway Enrichment Analysis.* In order to obtain a more comprehensive and in-depth knowledge of those chosen DEGs, GO function and KEGG pathway enrichment analysis were employed via DAVID. After importing all the DEGs to the DAVID software, we discovered upregulated DEGs and downregulated DEGs by GO analysis. To be more specific, these DEGs were mainly enriched in biological processes (BP), involving epoxygenase P450 pathway; oxidation-reduction process; cellular response to zinc ion; negative regulation of growth; and exogenous drug catabolic process for downregulation, mitotic nuclear division, cell division, sister chromatid cohesion, chromosome segregation, and protein localization to kinetochore for upregulation. As for function (MF), the downregulated DEGs were mainly implicated with oxidoreductase activity (acting on paired donors, with incorporation or reduction of molecular oxygen), oxygen binding, iron ion binding, monooxygenase activity, and oxidoreductase activity (acting on paired donors, with incorporation or reduction of molecular oxygen, reduced flavin or flavoprotein as one donor, and incorporation of one atom of oxygen). The upregulated DEGs were mainly responsible for protein binding, microtubule motor activity, microtubule binding, chromatin binding, and cyclin-dependent protein serine/threonine kinase activity. In addition, GO cell component (CC) analysis uncovered that the downregulated DEGs were principally enriched in the extracellular region, extracellular space, organelle membrane, integral component of plasma membrane, and basolateral plasma membrane, while the upregulated DEGs were mainly enriched in midbody, kinetochore, condensed chromosome kinetochore, chromosome, centromeric region, as well as kinesin complex (Table 2).

Table 3 displayed the most significantly enriched KEGG pathway of the upregulated and downregulated DEGs. These downregulated DEGs were enriched in mineral absorption, retinol metabolism, caffeine metabolism, drug metabolism-Cytochrome P450, and chemical carcinogenesis, while the upregulated DEGs were enriched in cell cycle, p53 signaling pathway, progesterone-mediated oocyte maturation, and
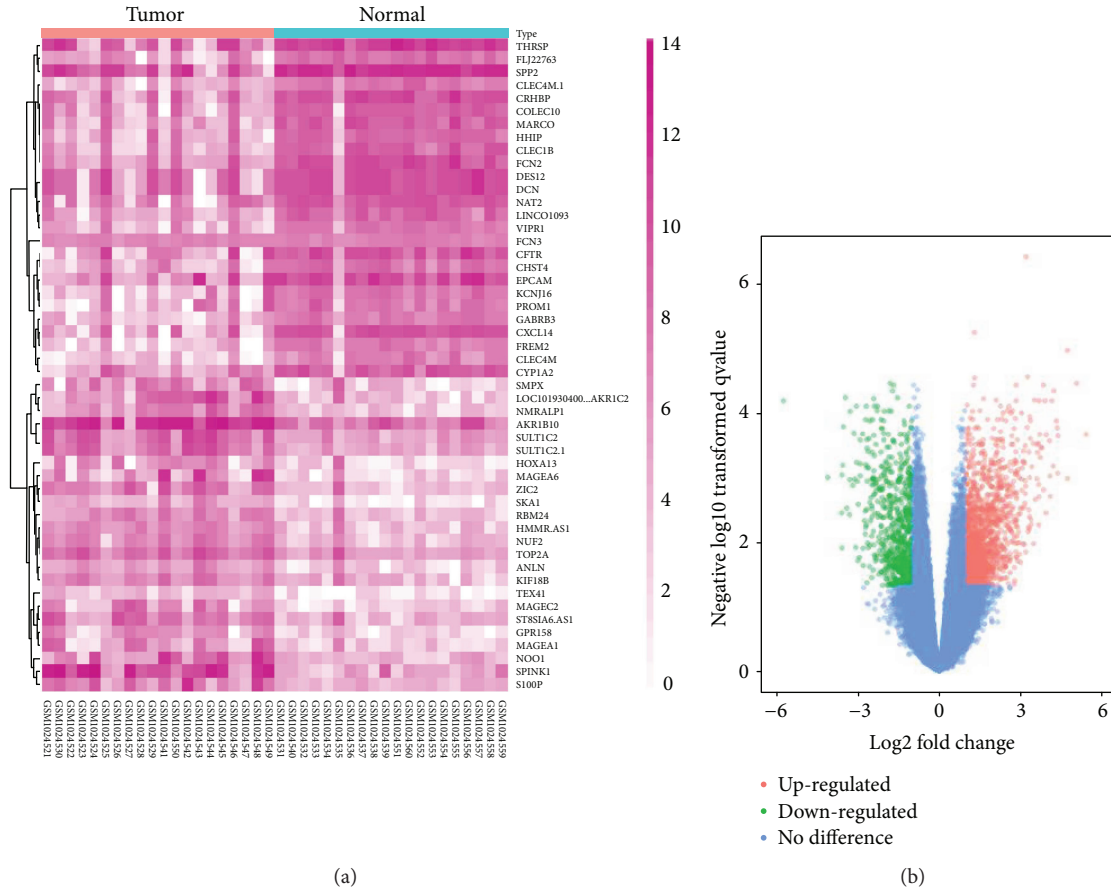
(a)



(b)

Figure 1: (a) Heat map of 50 representative DEGs. (b) Volcano plot of genes detected in HCC. Red means upregulated DEGs; green means downregulated DEGs; blue means no difference.

Table 1: Top 15 hub genes with higher degree of connectivity.

| Gene | Degree of connectivity | Adjusted $P$ value |
|------|----------------------|--------------------|
| TOP2A | 48 | $2.13E - 04$ |
| CDK1 | 43 | $1.87E - 03$ |
| CCNB1 | 42 | $3.57E - 04$ |
| BUB1 | 42 | $1.31E - 03$ |
| CENPF | 41 | $2.23E - 04$ |
| CCNB2 | 40 | $3.11E - 04$ |
| TTK | 40 | $1.06E - 03$ |
| KIF2C | 40 | $5.80E - 03$ |
| HMMR | 40 | $2.10E - 04$ |
| MELK | 40 | $9.21E - 04$ |
| CENPE | 39 | $2.49E - 03$ |
| KIF20A | 39 | $1.33E - 04$ |
| KIF4A | 39 | $4.66E - 04$ |
| PBK | 39 | $1.07E - 03$ |
| DLGAP5 | 39 | $1.01E - 03$ |

oocyte meiosis. Figures 2(a)–2(c) gives a GO and KEGG pathway enrichment plot of HCC.

3.3. *Hub Genes and Module Screening from the PPI Network.* Based on the information of the STRING protein query from public databases, we constructed the PPI network of the top 15 hub genes according to the degree of connectivity (Figure 2(d)). The top 15 hub genes with a higher degree of connectivity are as follows: TOP2A, CDK1, CCNB1, BUB1, CENPF, CCNB2, TTK, KIF2C, HMMR, MELK,CENPE, KIF20A, KIF4A, PBK, and DLGAP5. By the Kaplan-Meier plotter, we found that a total of 14 hub genes contributed to worse overall survival situation except CCNB2. Again, based on the GO function, KEGG pathway analysis, and the survival analysis, we unveiled that CCNB1, CDK1, BUB1, and TTK were enriched in cell cycle.

In order to detect the most significant modules in this PPI network, we employed the MCODE plug-in. The top 3 modules were selected (Figure 3). KEGG pathway analysis disclosed that the top 3 modules were mainly associated with cell cycle, oxidative stress, and liver detoxification (Table 4).

3.4. *The Kaplan-Meier Plotter and Expression Level of Hub Genes.* We obtained the prognostic information of the top

Table 2: Gene ontology analysis of differentially expressed genes associated with hepatocellular carcinoma.

| Expression | Category | Term | Count | % | $P$ value | FDR |
|---|---|---|---|---|---|---|
| Downregulated | GOTERM_BP_DIRECT | GO:0019373~epoxygenase P450 pathway | 7 | 0.02 | $5.20E-08$ | $8.49E-05$ |
| | GOTERM_BP_DIRECT | GO:0055114~oxidation-reduction process | 26 | 0.09 | $7.31E-08$ | $1.19E-04$ |
| | GOTERM_BP_DIRECT | GO:0071294~cellular response to zinc ion | 7 | 0.02 | $7.53E-08$ | $1.23E-04$ |
| | GOTERM_BP_DIRECT | GO:0045926~negative regulation of growth | 7 | 0.02 | $7.53E-08$ | $1.23E-04$ |
| | GOTERM_BP_DIRECT | GO:0042738~exogenous drug catabolic process | 6 | 0.02 | $1.95E-07$ | $3.19E-04$ |
| | GOTERM_CC_DIRECT | GO:0005576~extracellular region | 54 | 0.18 | $2.46E-12$ | $3.08E-09$ |
| | GOTERM_CC_DIRECT | GO:0005615~extracellular space | 44 | 0.14 | $1.19E-09$ | $1.49E-06$ |
| | GOTERM_CC_DIRECT | GO:0031090~organelle membrane | 12 | 0.04 | $5.53E-09$ | $6.91E-06$ |
| | GOTERM_CC_DIRECT | GO:0005887~integral component of plasma membrane | 41 | 0.14 | $1.42E-07$ | $1.77E-04$ |
| | GOTERM_CC_DIRECT | GO:0016323~basolateral plasma membrane | 12 | 0.04 | $9.02E-06$ | 0.01 |
| | GOTERM_MF_DIRECT | GO:0016705~oxidoreductase activity, acting on paired donors, with incorporation or reduction of molecular oxygen | 10 | 0.03 | $2.41E-08$ | $3.42E-05$ |
| | GOTERM_MF_DIRECT | GO:0019825~oxygen binding | 9 | 0.03 | $8.01E-08$ | $1.14E-04$ |
| | GOTERM_MF_DIRECT | GO:0005506~iron ion binding | 13 | 0.04 | $3.31E-07$ | $4.70E-04$ |
| | GOTERM_MF_DIRECT | GO:0004497~monooxygenase activity | 9 | 0.03 | $4.36E-07$ | $6.19E-04$ |
| | GOTERM_MF_DIRECT | GO:0016712~oxidoreductase activity, acting on paired donors, with incorporation or reduction of molecular oxygen, reduced flavin or flavoprotein as one donor, and incorporation of one atom of oxygen | 6 | 0.02 | $6.52E-07$ | $9.26E-04$ |
| Upregulated | GOTERM_BP_DIRECT | GO:0007067~mitotic nuclear division | 19 | 16.67 | $5.25E-15$ | $7.80E-12$ |
| | GOTERM_BP_DIRECT | GO:0051301~cell division | 19 | 16.67 | $1.94E-12$ | $2.90E-09$ |
| | GOTERM_BP_DIRECT | GO:0007062~sister chromatid cohesion | 12 | 10.53 | $2.16E-11$ | $3.23E-08$ |
| | GOTERM_BP_DIRECT | GO:0007059~chromosome segregation | 8 | 7.02 | $1.44E-07$ | $2.16E-04$ |
| | GOTERM_BP_DIRECT | GO:0034501~protein localization to kinetochore | 4 | 3.51 | $2.31E-05$ | 0.03 |
| | GOTERM_CC_DIRECT | GO:0030496~midbody | 10 | 0.06 | $2.85E-08$ | $3.40E-05$ |
| | GOTERM_CC_DIRECT | GO:0000776~kinetochore | 8 | 0.05 | $2.45E-07$ | $2.93E-04$ |
| | GOTERM_CC_DIRECT | GO:0000777~condensed chromosome kinetochore | 7 | 0.04 | $6.94E-06$ | 0.01 |
| | GOTERM_CC_DIRECT | GO:0000775~chromosome, centromeric region | 6 | 0.03 | $1.29E-05$ | 0.02 |
| | GOTERM_CC_DIRECT | GO:0005871~kinesin complex | 5 | 0.03 | $1.81E-04$ | 0.22 |
| | GOTERM_MF_DIRECT | GO:0005515~protein binding | 72 | 63.16 | $4.54E-06$ | 0.01 |
| | GOTERM_MF_DIRECT | GO:0003777~microtubule motor activity | 5 | 4.39 | 0.001073553 | 1.34 |
| | GOTERM_MF_DIRECT | GO:0008017~microtubule binding | 6 | 5.26 | 0.006401849 | 7.77 |
| | GOTERM_MF_DIRECT | GO:0003682~chromatin binding | 8 | 7.02 | 0.006540341 | 7.93 |
| | GOTERM_MF_DIRECT | GO:0004693~cyclin-dependent protein serine/threonine kinase activity | 3 | 2.63 | 0.015639967 | 18.01 |

GO: gene ontology; FDR: false discovery rate.

15 hub genes in http://gepia.cancer-pku.cn/. It was demonstrated that expression of TOP2A (HR (high) = 0.003, logrank $P = 0.0028$) was associated with worse overall survival (OS) for HCC patients, as well as CDK1(HR (high) = 0.00022, logrank $P = 0.00017$), CCNB1 (HR (high) = 2E − 04, logrank $P = 0.00015$), BUB1 (HR (high) = 0.0012, logrank $P = 0.001$), CENPF (HR (high) = 0.0018, logrank $P = 0.002$), TTK (HR (high) = 0.015, logrank $P = 0.0017$), KIF2C (HR (high) = 1.1E − 05, logrank $P = 1.7E − 05$), HMMR (HR (high) = 0.0031, logrank $P = 0.0035$), MELK(HR (high) = 0.0015, logrank $P = 0.0017$), CENPE(HR (high) = 0.011, logrank $P = 0.012$), KIF20A (HR (high) = 0.0034, logrank $P = 0.037$), KIF4A (HR (high) = 0.001, logrank $P = 0.0012$), and DLGAP5(HR (high) = 0.00039, Logrank $P = 0.00049$). Only the level of CCNB2 (HR (high) = 0.053, logrank $P = 0.052$) had no obvious difference on the survival curve of HCC patients (Figure 4).

Then, we selected 4 hub genes based on the KEGG pathways (Table 5) of the top 15 genes to verify the expression level in liver tissues between HCC and healthy people using GEPIA, and Figures 5(a)–5(d) showed that compared to normal group, the expression level of TOP2A, CCNB1, KIF4A, and CCNB2 significantly elevated in HCC patients. Intriguingly, CCNB2 in fact had no influence on the prognosis of HCC patients. Subsequently, we searched the immunohistochemical data in the HPA website. (The protein

TABLE 3: KEGG pathway analysis of differentially expressed genes associated with hepatocellular carcinoma.

| Category | Term | Count | % | P value | Genes | FDR |
|---|---|---|---|---|---|---|
| Downregulated DEGs | hsa04978: mineral absorption | 9 | 0.03 | $2.22E-07$ | MT1M, SLC5A1, MT2A, MT1E, TRPV6, MT1H, MT1X, MT1G, and MT1F | $2.68E-04$ |
| | hsa00830: retinol metabolism | 10 | 0.03 | $2.90E-07$ | CYP3A4, CYP4A11, CYP2B6, CYP2C8, ADH4, ADH1B, CYP26A1, CYP2A6, CYP1A2, and RDH16 | $3.50E-04$ |
| | hsa00232: caffeine metabolism | 4 | 0.01 | $2.79E-05$ | XDH, NAT2, CYP2A6, and CYP1A2 | 0.03 |
| | hsa00982: drug metabolism-cytochrome P450 | 8 | 0.03 | $4.75E-05$ | CYP3A4, CYP2B6, CYP2C8, ADH4, ADH1B, CYP2A6, CYP2E1, and CYP1A2 | 0.06 |
| | hsa05204: chemical carcinogenesis | 8 | 0.03 | $1.35E-04$ | CYP3A4, CYP2C8, ADH4, NAT2, ADH1B, CYP2A6, CYP2E1, and CYP1A2 | 0.16 |
| Upregulated DEGs | hsa04110: cell cycle | 8 | 0.05 | $9.30E-07$ | CCNB1, CDK1, CCNB2, BUB1, TTK, PTTG1, SFN, and CDC25C | $9.18E-04$ |
| | hsa04115: p53 signaling pathway | 6 | 0.04 | $1.03E-05$ | CCNB1, CDK1, CCNB2, RRM2, SFN, and GTSE1 | 0.01 |
| | hsa04914: progesterone-mediated oocyte maturation | 5 | 0.03 | $5.69E-04$ | CCNB1, CDK1, CCNB2, BUB1, and CDC25C | 0.56 |
| | hsa04114: oocyte meiosis | 4 | 0.03 | 0.01 | CDK1, BUB1, PTTG1, and CDC25C | 11.64 |

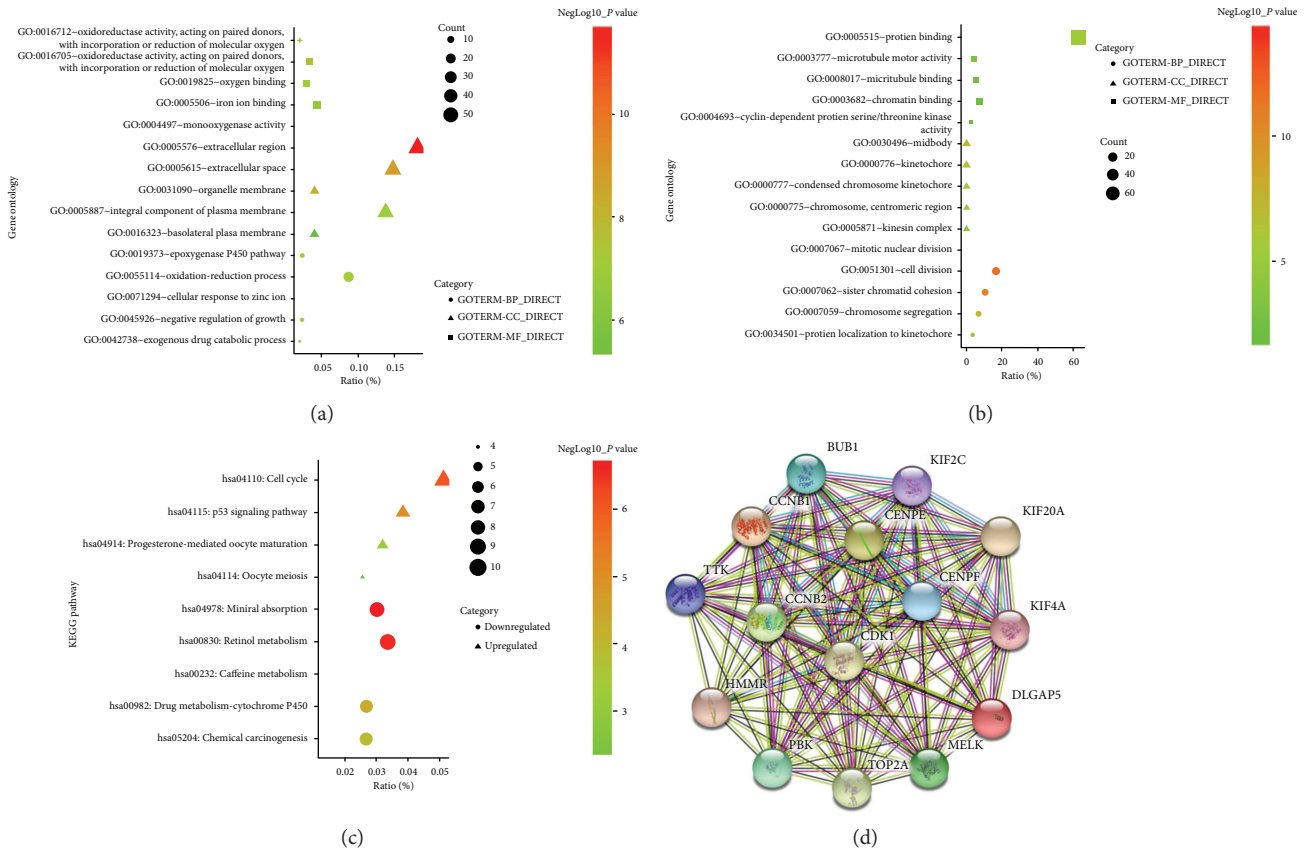KEGG: Kyoto Encyclopedia of Genes and Genomes; FDR: false discovery rate.



FIGURE 2: (a) GO analysis of downregulated DEGs. (b) GO analysis of upregulated DEGs. (c) KEGG pathway of DEGs. (d) The protein-protein interaction (PPI) network of the top 15 hub genes.
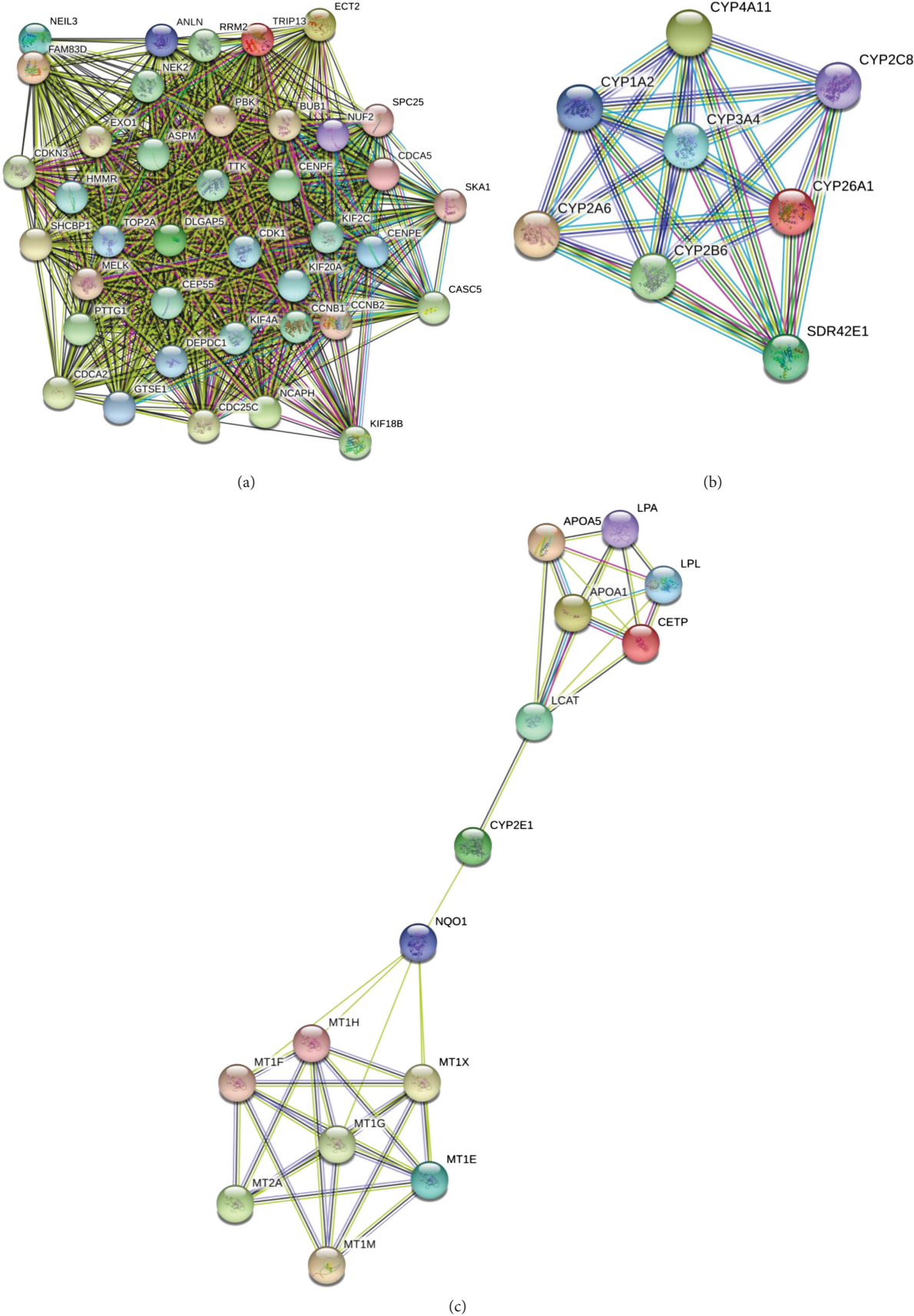
(a)

(b)

(c)

FIGURE 3: Top 3 modules from the protein-protein interaction network: (a) module 1, (b) module 2, and (c) module 3.

TABLE 4: The enriched pathways of top 3 modules.

| Module | Term | $P$ value | FDR | Genes |
|---|---|---|---|---|
| Module 1 | Cell cycle | $2.66E-08$ | $1.96E-05$ | CCNB1, CDK1, CCNB2, BUB1, TTK, PTTG1, and CDC25C |
| | ATP binding | $3.86E-07$ | $3.59E-04$ | CDK1, KIF4A, NEK2, KIF18B, TTK, CENPE, PBK, KIF2C, BUB1, TOP2A, MELK, TRIP13, and KIF20A |
| | Kinesin, motor region, and conserved site | $1.54E-06$ | 0.0016579 | KIF2C, KIF4A, KIF18B, CENPE, and KIF20A |
| | Kinesin, motor domain | $2.30E-06$ | 0.00247205 | KIF2C, KIF4A, KIF18B, CENPE, and KIF20A |
| | p53 signaling pathway | $3.59E-06$ | 0.002649002 | CCNB1, CDK1, CCNB2, RRM2, and GTSE1 |
| Module 2 | Cytochrome P450, conserved site | $4.98E-15$ | $3.11E-12$ | CYP3A4, CYP4A11, CYP2B6, CYP2C8, CYP26A1, CYP2A6, and CYP1A2 |
| | Cytochrome P450 | $9.23E-15$ | $5.74E-12$ | CYP3A4, CYP4A11, CYP2B6, CYP2C8, CYP26A1, CYP2A6, and CYP1A2 |
| | Monooxygenase | $3.58E-14$ | $2.84E-11$ | CYP3A4, CYP4A11, CYP2B6, CYP2C8, CYP26A1, CYP2A6, and CYP1A2 |
| | Organelle membrane | $6.92E-14$ | $3.79E-11$ | CYP3A4, CYP4A11, CYP2B6, CYP2C8, CYP26A1, CYP2A6, and CYP1A2 |
| | Metal ion-binding site: iron (heme axial ligand) | $8.64E-14$ | $6.13E-11$ | CYP3A4, CYP4A11, CYP2B6, CYP2C8, CYP26A1, CYP2A6, and CYP1A2 |
| Module 3 | Metal-thiolate cluster | $2.15E-17$ | $1.80E-14$ | MT1M, MT2A, MT1E, MT1H, MT1G, MT1X, MT1F |
| | Metallothionein, vertebrate, and metal binding site | $2.35E-17$ | $1.91E-14$ | MT1M, MT2A, MT1E, MT1H, MT1G, MT1X, and MT1F |
| | Metallothionein, vertebrate | $5.17E-17$ | $4.19E-14$ | MT1M, MT2A, MT1E, MT1H, MT1G, MT1X, and MT1F |
| | Metallothionein domain | $5.17E-17$ | $4.19E-14$ | MT1M, MT2A, MT1E, MT1H, MT1G, MT1X, and MT1F |
| | Metallothionein superfamily, eukaryotic | $5.17E-17$ | $4.19E-14$ | MT1M, MT2A, MT1E, MT1H, MT1G, MT1X, and MT1F |

expression of CCNB2 was absent in HPA.) The staining pictures demonstrated that the TOP2A, CCNB1, and KIF4A in HCC patients exhibited higher expression levels compared with those in healthy individuals, which further verified the results of boxplots from GEPIA (Figure 5(e)).

Finally, we selected two most suspicious genes (CCNB1 and CDK1) based the KEGG analysis of the top 15 hub genes. CCNB1 and CDK1 were two genes which were implicated with cell cycle, progesterone-mediated oocyte maturation, and p53 signaling pathway (Table 5). Using the correlation analysis in GEPIA, we found that CCNB1 and CDK1 are obviously positively correlated ($P$ value = 0, $R = 0.77$) (Figure 5(f)).

3.5. Gene Set Enrichment Analysis. To acquire further insight into the function of the hub gene, GSEA was conducted to map into GO analysis and KEGG pathways database. Under the cut-off criteria FDR < 0.05, |enrichment score (ES)| > 0.6, and gene size ≥ 100, a total of 6 functional gene sets were enriched, which mainly focused on pathways associated with cell proliferation and differentiation. The six pathways were "spindle assembly," "spindle," "negative regulation of mitotic nuclear division," "spindle microtubule," "cytoskeleton dependent cytokinesis," and "regulation of sulfur metabolic process" (Figure 6).

3.6. Oxidative Stress Is Activated in HCC. Consistent with what we have predicted, the level of oxidative stress was significantly enhanced in carcinoma tissue compared with adjacent tissue. In detail, the activity of SOD, one of the typical antioxidant enzymes, was decreased in carcinoma tissue while the activity of GSH-Px as well as the level of MDA were increased in carcinoma tissue (Figure 7(a)). Meanwhile, the mRNA level of NADPH P67 and gp91 were also significantly upregulated in the HCC tissue (Figure 7(b)). The results from the Western blot and immunohistochemical staining further identified the protein level of these biomarkers associated with oxidative stress (Figures 7(c)–7(e)). Taken together, our experiments demonstrated that oxidative stress was activated in HCC, which further proved our hypothesis from bioinformatics.

## 4. Discussion

Trends of HCC mortality rates have elevated over recent decades worldwide. Although the diagnostic and treatment approaches have developed a lot recently, the prognosis of HCC is still poor [20]. Thus, specific and sensitive biomarkers for HCC are urgently needed to be selected. High-throughput research can facilitate the in-depth exploration of the vital mechanisms contributing to HCC. Our study systematically focused on expression profiling obtained from microarray studies of HCC. Our analysis included 20 HCC samples and 20 normal samples from the GEO database of GSE41804. A total of 503 DEGs were captured involving 360 upregulated genes and 143 downregulated genes. To have a better exploration of these DEGs, we carried out GO function and KEGG pathway analysis of these DEGs.
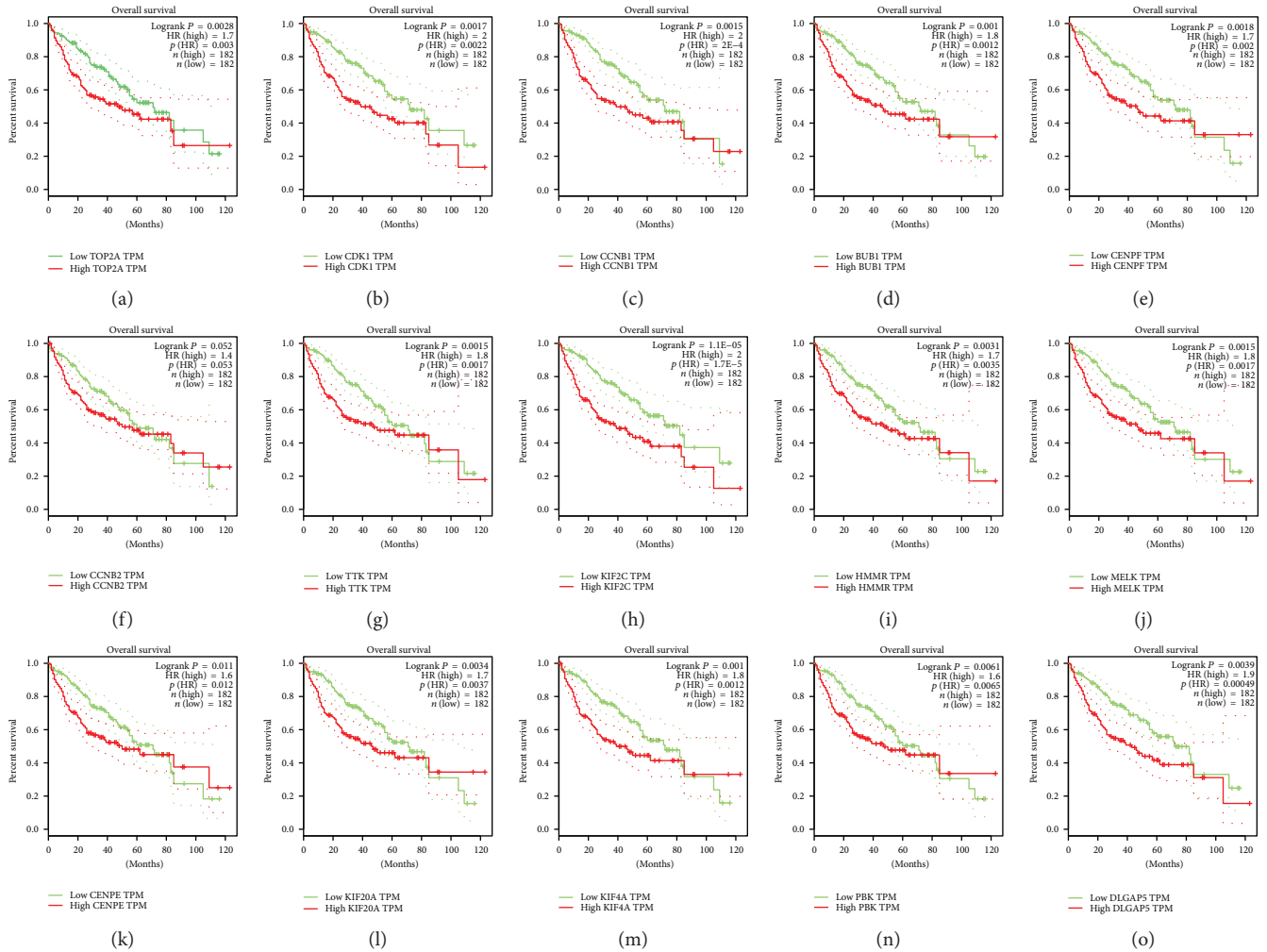
FIGURE 4: Prognostic value of 15 genes ((a) TOP2A, (b) CDK1, (c) CCNB1, (d) BUB1, (e) CENPF, (f) CCNB2, (g) TTK, (h) KIF2C, (i) HMMR, (j) MELK, (k) CENPE, (l) KIF20A, (m) KIF4A, (n) PBK, and (o) DLGAP5) in HCC. $P < 0.05$ was regarded statistically different.

### 4.1. Oxidative Stress Is Critical in the Carcinogenesis of HCC.

Although many mechanisms have been disclosed to contribute to the progression of HCC, the predominant mechanism implicated with tumorigenesis is still controversial, which brings some difficulties to the diagnosis and treatment of HCC. Gene ontology and PPI analysis in our study showed that downregulated DEGs were primarily involved in oxidative stress. Our experimental results in carcinoma tissue and adjacent tissue further identified the vital role of oxidative stress in HCC.

To our knowledge, oxidative stress is recognized to play a vital part in the initiation and promotion of carcinogenesis because it can occur and overproduce ROS and RNS through endogenous or exogenous insults [21]. On the one hand, for the reason that polymorphonuclear neutrophils (PMNs) are a major source of ROS in an inflamed liver, oxidative stress acts as a core player in the pathogenesis of chronic liver diseases and precancerous lesions infected by hepatitis B virus (HBV) or hepatitis C virus (HCV) [22]. On the other one hand, nonparenchymal cells including macrophages and Kupffer cells, which can release cytokines, are another

incentive of ROS production in hepatocytes [23]. To be more specific, prolonged or upregulated ROS production is associated with modification and mutation of gene expression in HCC. Particularly, unrepaired damage induced by oxidative stress to DNA could give rise to mutations, given that the repair of modified bases ensues later than cell replication. Apart from oxidative nuclear DNA damage, formation of mitochondrial DNA damage or mutation as well as alteration of mitochondrial genomic function have also been unveiled to induce the occurrence of carcinogenesis [3, 24]. Thus, the level of oxidative stress can be a promising predictor in the diagnosis and treatment of HCC.

Additionally, our gene ontology analysis indicated that the downregulated DEGs were primarily related with the alteration of extracellular structure including extracellular space, organelle membrane, integral component of plasma membrane, and basolateral plasma membrane. Increased extracellular matrix remodeling has also been proved to be associated with tumor progression in human HCC. For instance, matrix metalloproteinase-2 (MMP-2) is an important enzyme in the process of extracellular matrix

TABLE 5: KEGG pathway analysis of top 15 hub genes with higher degree of connectivity.

| Term | Count | % | $P$ value | Genes | FDR |
|---|---|---|---|---|---|
| cfa04110: cell cycle | 5 | 0.18 | $5.08E - 07$ | CCNB1, CDK1, CCNB2, BUB1, and TTK | $3.05E - 04$ |
| cfa04914: progesterone-mediated oocyte maturation | 4 | 0.15 | $1.93E - 05$ | CCNB1, CDK1, CCNB2, and BUB1 | 0.01 |
| cfa04115: p53 signaling pathway | 3 | 0.11 | $8.88E - 04$ | CCNB1, CDK1, and CCNB2 | 0.53 |
| cfa04114: oocyte meiosis | 2 | 0.07 | 0.07 | CDK1, BUB1 | 37.98 |
| cfa04068: FoxO signaling pathway | 2 | 0.07 | 0.09 | CCNB1, CCNB2 | 44.34 |

KEGG: Kyoto Encyclopedia of Genes and Genomes; FDR: false discovery rate.

remodeling implicated with tumor invasion and metastasis. Overexpression of MMP2 seemed strikingly associated with HCC because MMP2 in the tumor is mainly responsible for the fibrogenesis [25]. As reported, hepatic stellate cells, acting as main connective tissue cells in the liver, could be activated by oxidative stress and then produce extracellular matrix which is essential for normal growth and differentiation of cells after liver damage [26]. Our result suggests that oxidative stress in HCC not only directly affects the progression of HCC, but also interacts with other events to modulate HCC.

What is more, KEGG analysis shows that the upregulated DEGs are implicated with p53 signaling. Our data from Western blot also identified that the expression of P-p53 in HCC tissue was significantly higher than that in adjacent tissue. To our knowledge, p53 genes are one of the sensitive redox transcription factor which could be upregulated by enhancing its translational speed and posttranslational modification when the DNA is damaged by oxidative stress in cells. The posttranslational modification of oxidative stress in cell, such as phosphorylation, ubiquitination, sumoylation, acetylation, and methylation, may cause conformational and locational changes of p53 and then affect its downstream targets [27, 28]. Taken together, strategies to suppress the alteration of oxidative stress or regulate various posttranscriptional modifications of p53 and formation of extracellular matrix through oxidative stress are helpful to develop drugs for the treatment of HCC.

### 4.2. Targeting Cell Cycle Could Be a Potential Strategy for Therapy of HCC.

Dysregulated cell cycle-mediated cell transformation and uncontrolled cell growth are some of the fundamental biological features of malignant tumors. Amplification of cyclin genes, especially cyclins D and E, is a crucial event process which occurs in the HCC [29, 30]. Masaki et al. found that in Long-Evans Cinnamon (LEC) rats, with the progression of HCC, cyclin D1-related kinase activities were dramatically enhanced, in particular, the cyclin D1-related enzymatic activity. On the contrary, the activity was relatively low in the 2-month-old LEC rats as well as in the control rats [31]. The top 15 hub genes with a higher degree of connectivity in our analysis demonstrated the significance of cell cycle in the progression of HCC. Most of these hub genes including CDK1 [32], CENPF [33], CCNB2 [34], MELK [35], CENPE [36], KIF20A [37], KIF4A [38], PBK [39], and DLGAP5 [40] have been proven to be responsible for the cell

cycle-associated proliferation and differentiation of tumor. Additionally, GO analysis of DEGs showed that all upregulated DEGs were also involved in cell cycle including mitotic nuclear division, cell division, sister chromatid cohesion, midbody, protein localization to kinetochore, and microtubule binding, which indicated that the altered expression of vital genes in HCC should be associated with cell cycle. KEGG pathway analysis further verified the hypothesis with the downregulated DEGs associated with cell cycle and p53 signaling pathway. Taken together, from our perspective based on the GO and KEGG analysis, drugs targeting the cell cycle of cancer cells may be a potential strategy for therapy of HCC.

### 4.3. Altered Cell Cycle, Dysfunction of Cytochrome P450, and Impaired Liver Detoxification Effect Are 3 Typical Modules in PPI Network for HCC.

PPI is defined as the process by which two or more kinds of protein molecules form a protein complex by noncovalent bonding. The PPI network could provide a visible framework for a better understanding of the functional organization of the proteome [41]. From the enriched pathways of top 3 modules, we uncovered that the interactions among the proteins in HCC mainly concentrated on pathways implicated with cell cycle, Cytochrome P450, and liver detoxification.

Cytochrome P450 is a big family of enzymes localizing to either the endoplasmic reticulum or mitochondrial membranes, which exert various important roles in the process of metabolizing endogenous and exogenous molecules, especially some drugs [42]. Previous studies have shown that Cytochrome P450 genetic polymorphisms exhibited a certain association with the risk of HCC in patients carrying chronic hepatitis B [43]. In HCC patients, the levels of some Cytochrome P450 also changed with the progression of HCC. For instance, CYP2J2, a member in Cytochrome P450 family, was discovered to have critical roles in the proliferation and resistance to the anticancer drug (doxorubicin) in HepG2 cells by decreasing the ratio of Bax/Bcl622 ratio and elevating pro62caspase623 levels [44]. Genetic polymorphisms of some Cytochrome P450 enzymes, such as CYP2D6*10, have been proven to have influence on enzyme activity. In HCC patients, CYP2D6*10 allelic frequency was obviously different compared with the control individuals [45]. Consistent with these findings, module 2 showed that the PPI in tumor groups and normal groups involved many members in Cytochrome P450, such as CYP3A4, CYP4A11, CYP2B6,
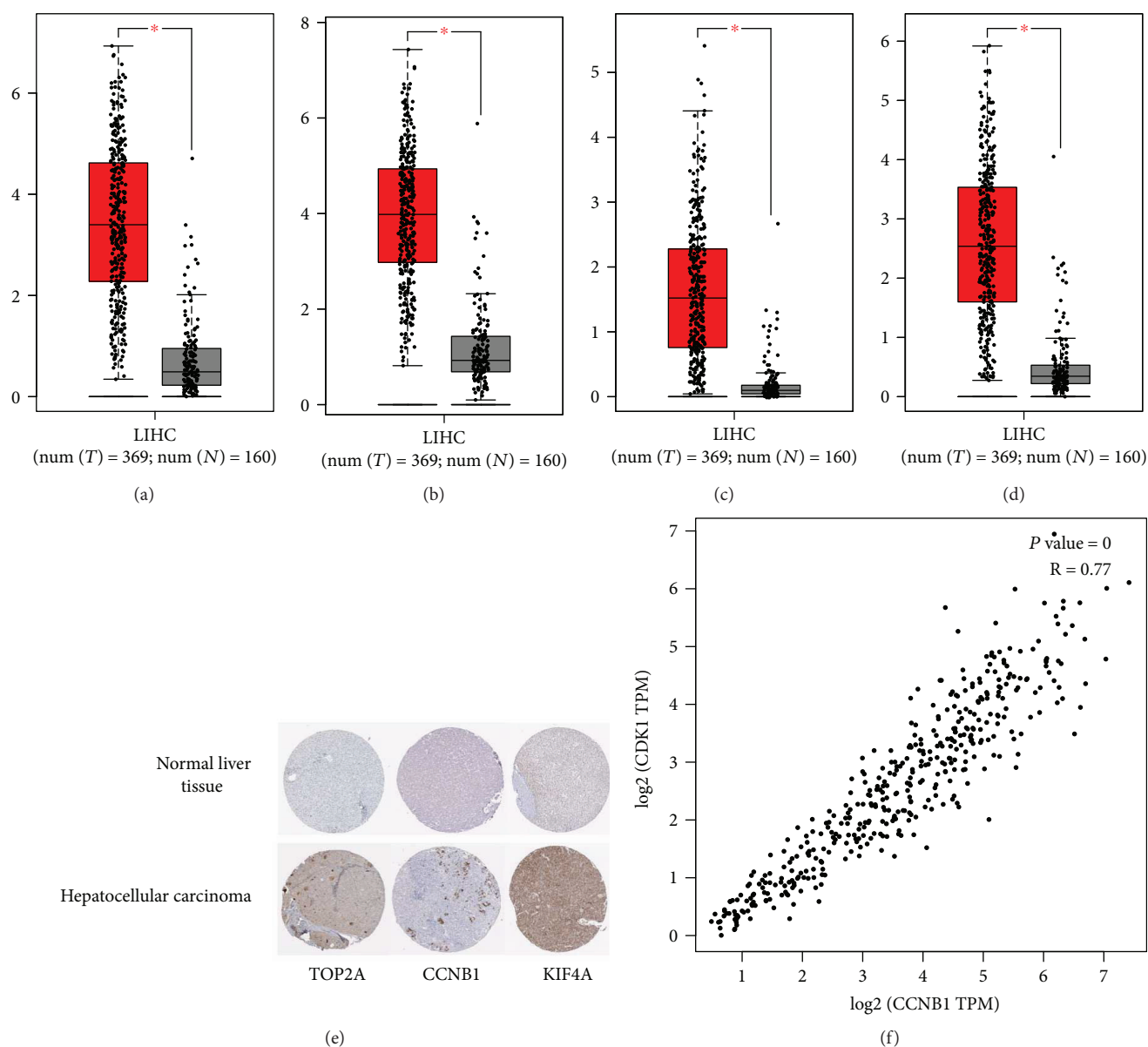
FIGURE 5: (a–d) Expression level of TOP2A, CCNB1, KIF4A, and CCNB2 in HCC and normal tissues. Number ($T = 369$, $N = 160$); $^*P < 0.05$. (e) TOP2A, CCNB1, and KIF4A protein were strongly upregulated in HCC tissues compared with normal liver tissues based on The Human Protein Atlas database. The normal liver tissue of TOP2A was from a female, aged 32, (patient ID: 1846; staining: not detected; intensity: negative; quantity: negative; location: none), and the HCC tissue was from a male, aged 80 (patient ID: 2280; staining: low; intensity: moderate; quantity: <25%; location: cytoplasmic/membranous nuclear). The normal liver tissue of CCNB1 was from a female, ages 63, (patient ID: 3222; staining: not detected; intensity: negative; quantity: negative; location: none), and the HCC tissue was from a female, aged 41, (patient ID: 5037; staining: moderate; intensity: weak; quantity: <25%; location: cytoplasmic/membranous nuclear). The normal liver tissue of KIF4A was from a female, aged 54 (patient ID: 3402; staining: not detected; intensity: negative; quantity: negative; location: none), and the HCC tissue was from a male, aged 67, (patient ID: 3477; staining: moderate; intensity: moderate; quantity: >75%; location: cytoplasmic/membranous nuclear). (f) The correlation analysis between CCNB1 and CDK1. CCNB1 and CDK1 are obviously positively correlated.

CYP2C8, CYP26A1, CYP2A6, and CYP1A2, indicating that some key Cytochrome P450 enzymes had essential functions in HCC.

In addition, metallothionein is also involved in the differentiation and proliferation of tumor cells. The relationship between metallothionein and tumors mainly focused on the metallothionein and tumorigenesis, toxic side effects of anti-tumor drugs, as well as drug resistance. Metallothionein expression defect is one of the symptoms of cancer; therefore, the in-depth study of the relationship between metallothionein and tumors is expected to obtain the target drugs for the treatment of cancer [46]. Metallothionein is expressed at a high level in liver tissues, which is mainly responsible for liver detoxification and can be significantly induced by a
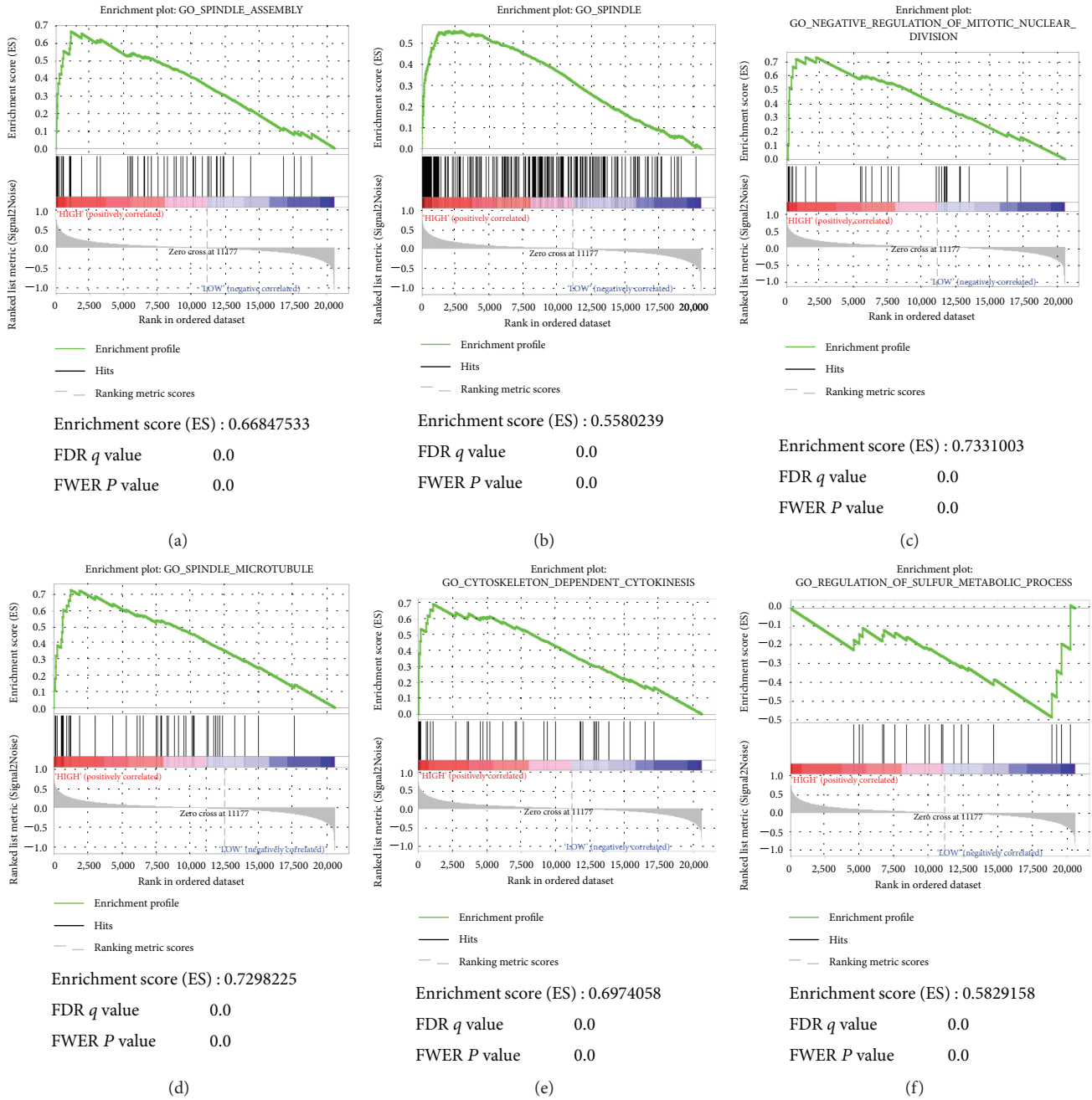
Figure 6: Gene set enrichment analysis (GSEA). Listed pictures are 10 representative functional gene sets enriched in HCC with CCNB2 highly expressed.

variety of drugs [47]. Datta et al. [48] demonstrated that in hepatocarcinogenesis, the expression of metallothionein was significantly blocked through inactivation of CCAAT/ enhancer-binding protein $\alpha$ by phosphatidylinositol 3-kinase (PI3K) signaling pathway, which eventually caused poor liver detoxification. Base on module 3 from the PPI network, we found that the network mainly concentrated on metallothionein, suggesting the vital significance of metallothionein from the view of bioinformatics. Hence, monitoring some indexes associated with metallothionein is of great importance for the diagnosis and treatment of HCC.

*4.4. CCNB2 May Be One of the Switches of HCC but Cannot Promote Tumor Progression.* As the Kaplan-Meier plotter showed, the survival curve displayed no significant difference in HCC patients with low expression and high expression of CCNB2. Intriguingly, in the HCC group and healthy group, the expression of CCNB2 exhibited obvious difference in the box diagram.

To our knowledge, CCNB2 (Cyclin B2), which belelongs to one of the members in cyclin family proteins, has a core role in G2/M transition of tumor. CCNB2 has been found to be upregulated in many types of human tumors [49]. In Chinese
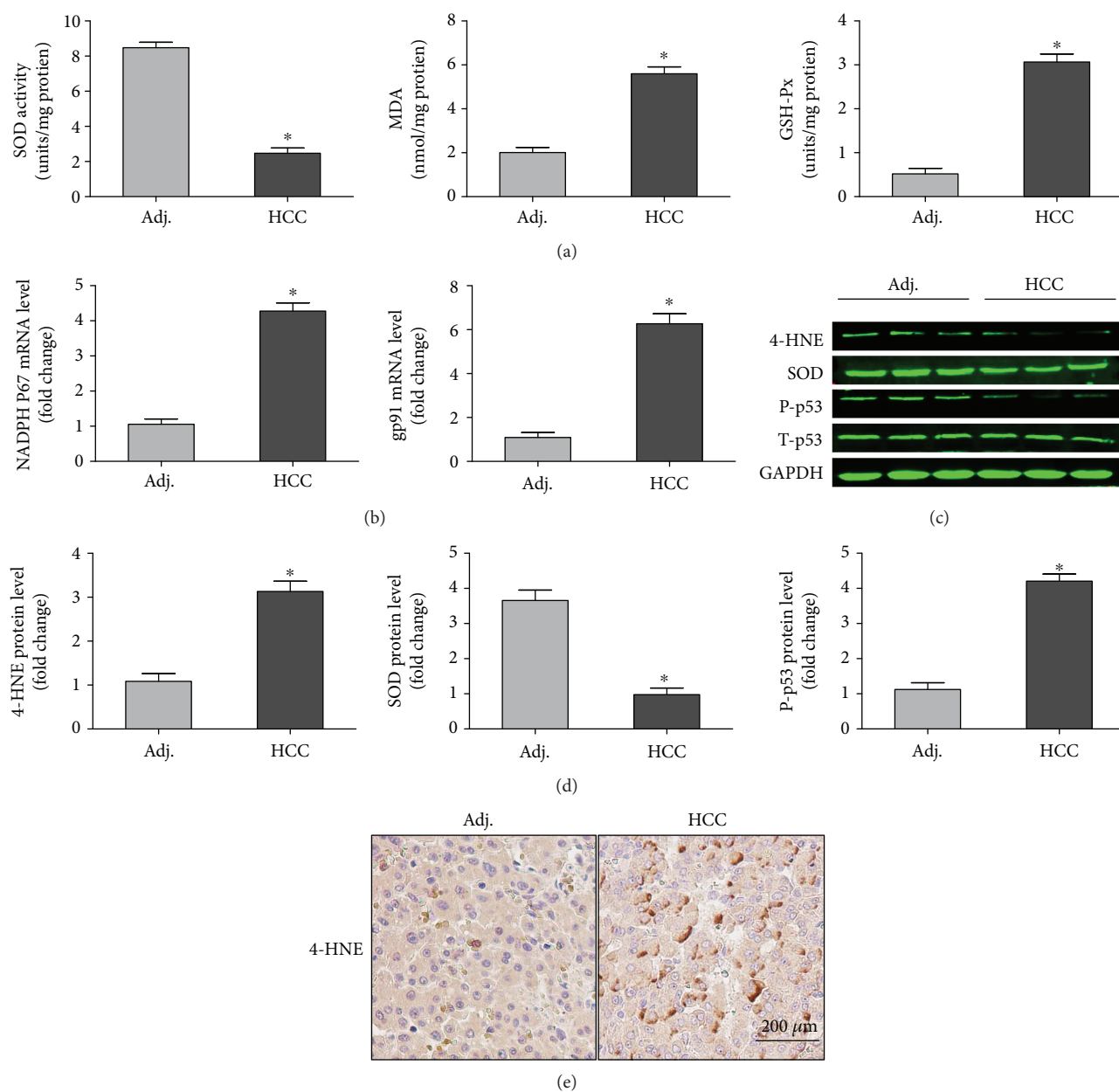
FIGURE 7: Reidentification of oxidative stress in HCC. (a) SOD activity, MDA production, and GSH-Px activity in the indicated group ($n = 6$). (b) The mRNA levels of NADPH P67 and gp91. ($n = 6$). (c, d) Western blotting analysis and quantitative data of oxidative stress ($n = 6$). (e) Representative images of immunohistochemical staining for the 4-HNE protein. $^*P < 0.05$ versus Adj. group. Adj: adjacent tissue; HCC: hepatocellular carcinoma.

non-small-cell lung cancer (NSCLC) patients, high expression levels of CCNB2 protein were positively correlated with the tumor size, status of differentiated degree, distant metastasis, lymph node metastasis, as well as clinical stage [50]. However, expression levels of CCNB2 do nothing with survival condition in HCC patients, while the levels of CCNB2 in HCC patients have obvious difference compared to the health group, which indicates that CCNB2 may act as a switch to initiate the occurrence of HCC, but it does not exert other tumor-related effects after the tumorigenesis. In fact, in the primary HCC tissue samples, CCNB2 has been unveiled to be regulated by its upstream karyopherin subunit-$\alpha$ 2, which can inhibit

cell proliferation and induce cell cycle arrest in the G2/M phase [34]. Based on GSEA, we also found that the gene sets associated with cell cycle-related pathways were enriched in the samples with FCER1G highly expressed HCC patients. But further study is required to clarify the process of CCNB2 transcriptional activation, the effect of CCNB2 on cell cycle progression, and how this affects initiation of HCC.

In conclusion, we offer a novel and comprehensive analysis of gene expression profiles to identify DEGs, which may play core roles in the occurrence, development, and prognosis in patients with HCC. Genes involved in oxidative stress and cell cycle, Cytochrome P450, and metallothionein were

significantly changed in HCC patients. To obtain more accurate correlation results, we intend to initiate subsequent identification experiments later to verify these predictive results. Taken together, we sincerely hope that this analysis will offer valuable and powerful information for future research on the molecular mechanisms contributing to HCC and provide clues for the discovery of novel diagnosis biomarkers and therapeutic strategies.

## Data Availability

The data used to support the findings of this study are available from the corresponding author upon request.

## Conflicts of Interest

All authors declare that they have no conflict of interests to state.

## Authors' Contributions

Ning Li and Ling Li contributed equally to this work.

## Acknowledgments

## References

[1] R. X. Zhu, W. K. Seto, C. L. Lai, and M. F. Yuen, "Epidemiology of hepatocellular carcinoma in the Asia-Pacific region," *Gut & Liver*, vol. 10, no. 3, pp. 332–339, 2016.

[2] K. Yamazaki, Y. Masugi, and M. Sakamoto, "Molecular pathogenesis of hepatocellular carcinoma: altering transforming growth factor-$\beta$ signaling in hepatocarcinogenesis," *Digestive Diseases*, vol. 29, no. 3, pp. 284–288, 2011.

[3] M. Marra, I. M. Sordelli, A. Lombardi et al., "Molecular targets and oxidative stress biomarkers in hepatocellular carcinoma: an overview," *Journal of Translational Medicine*, vol. 9, no. 1, p. 171, 2011.

[4] J. W. Jang, Y. Song, S. H. Kim et al., "CD133 confers cancer stem-like cell properties by stabilizing EGFR-AKT signaling in hepatocellular carcinoma," *Cancer Letters*, vol. 389, pp. 1–10, 2017.

[5] L. Cao, C. Li, S. Shen et al., "OCT4 increases BIRC5 and CCND1 expression and promotes cancer progression in hepatocellular carcinoma," *BMC Cancer*, vol. 13, no. 1, p. 82, 2013.

[6] W. Huang, Z. Chen, X. Shang et al., "Sox12, a direct target of FoxQ1, promotes hepatocellular carcinoma metastasis through up-regulating Twist1 and FGFBP1," *Hepatology*, vol. 61, no. 6, pp. 1920–1933, 2015.

[7] Y. Wang, M. C. Wu, J. S. Sham, W. Zhang, W. Q. Wu, and X. Y. Guan, "Prognostic significance of *c-myc* and *AIB1* amplification in hepatocellular carcinoma: A broad survey using high-throughput tissue microarray," *Cancer*, vol. 95, no. 11, pp. 2346–2352, 2002.

[8] T. Kalinski and A. Roessner, "Hepatocellular carcinoma: pathology and liver biopsy," *Digestive Diseases*, vol. 27, no. 2, pp. 102–108, 2009.

[9] M. Liu, Z. Xu, Z. Du et al., "The identification of key genes and pathways in glioma by bioinformatics analysis," *Journal of Immunology Research*, vol. 2017, Article ID 1278081, 9 pages, 2017.

[10] C. Sun, Q. Yuan, D. Wu, X. Meng, and B. Wang, "Identification of core genes and outcome in gastric cancer using bioinformatics analysis," *Oncotarget*, vol. 8, no. 41, pp. 70271–70280, 2017.

[11] L. Yuan, "Co-expression network analysis identified FCER1G in association with progression and prognosis in human clear cell renal cell carcinoma," *International Journal of Biological Sciences*, vol. 13, no. 11, pp. 1361–1372, 2017.

[12] A. Ward, A. Balwierz, J. D. Zhang et al., "Re-expression of microRNA-375 reverses both tamoxifen resistance and accompanying EMT-like properties in breast cancer," *Oncogene*, vol. 32, no. 9, pp. 1173–1182, 2013.

[13] S. Luo, N. Cao, T. Yao, and W. Gu, "Identification of key microRNAs and genes in preeclampsia by bioinformatics analysis," *PLoS One*, vol. 12, no. 6, article e0178549, 2017.

[14] P. Gaudet, N. Škunca, J. C. Hu, C. Dessimoz, C. Dessimoz, and N. Škunca, "Primer on the gene ontology," in *The Gene Ontology Handbook*, vol. 1446 of Methods in Molecular Biology, pp. 25–37, Humana Press, New York, NY, USA, 2017.

[15] M. Kanehisa, "The KEGG database," in *"In Silico" Simulation of Biological Processes*:, vol. 247, pp. 91–101, Novartis Foundation Symposium, 2002.

[16] D. W. Huang, B. T. Sherman, Q. Tan et al., "The DAVID gene functional classification tool: a novel biological module-centric algorithm to functionally analyze large gene lists," *Genome Biology*, vol. 8, no. 9, article R183, 2007.

[17] D. Szklarczyk, A. Franceschini, S. Wyder et al., "STRING v10: protein–protein interaction networks, integrated over the tree of life," *Nucleic Acids Research*, vol. 43, no. D1, pp. D447–D452, 2015.

[18] Z. Tang, C. Li, B. Kang, G. Gao, C. Li, and Z. Zhang, "GEPIA: a web server for cancer and normal gene expression profiling and interactive analyses," *Nucleic Acids Research*, vol. 45, no. W1, pp. W98–102, 2017.

[19] M. Uhlen, C. Zhang, S. Lee et al., "A pathology atlas of the human cancer transcriptome," *Science*, vol. 357, no. 6352, article eaan2507, 2017.

[20] W. Okajima, S. Komatsu, D. Ichikawa et al., "Liquid biopsy in patients with hepatocellular carcinoma: circulating tumor cells and cell-free nucleic acids," *World Journal of Gastroenterology*, vol. 23, no. 31, pp. 5650–5668, 2017.

[21] S. S. Thorgeirsson and J. W. Grisham, "Molecular pathogenesis of human hepatocellular carcinoma," *Toxicology*, vol. 181-182, pp. 43–47, 2002.

[22] F. Balkwill and A. Mantovani, "Inflammation and cancer: back to Virchow?," *The Lancet*, vol. 357, no. 9255, pp. 539–545, 2001.

[23] R. V. Lloyd, P. M. Hanna, and R. P. Mason, "The origin of the hydroxyl radical oxygen in the Fenton reaction," *Free Radical Biology and Medicine*, vol. 22, no. 5, pp. 885–888, 1997.

[24] H. Zhong, M. Xiao, K. Zarkovic et al., "Mitochondrial control of apoptosis through modulation of cardiolipin oxidation in hepatocellular carcinoma: a novel link between oxidative stress

and cancer," *Free Radical Biology and Medicine*, vol. 102, pp. 67–76, 2016.

[25] N. Théret, O. Musso, B. Turlin et al., "Increased extracellular matrix remodeling is associated with tumor progression in human hepatocellular carcinomas," *Hepatology*, vol. 34, no. 1, pp. 82–88, 2001.

[26] R. Urtasun and N. Nieto, "Hepatic stellate cells and oxidative stress," *Revista Espanola De Enfermedades Digestivas*, vol. 99, no. 4, pp. 223–230, 2007.

[27] P. Fuschi, M. Carrara, C. Voellenkle et al., "Central role of the p53 pathway in the noncoding-RNA response to oxidative stress," *Aging*, vol. 9, no. 12, pp. 2559–2586, 2017.

[28] K. Beyfuss and D. A. Hood, "A systematic review of p53 regulation of oxidative stress in skeletal muscle," *Redox Report Communications in Free Radical Research*, vol. 23, no. 1, pp. 100–117, 2018.

[29] W. Zhan, X. Liao, L. Yu et al., "Effects of blueberries on migration, invasion, proliferation, the cell cycle and apoptosis in hepatocellular carcinoma cells," *Biomedical Reports*, vol. 5, no. 5, pp. 579–584, 2016.

[30] H. Yu, H. L. Jiang, D. Xu et al., "Transcription factor MafB promotes hepatocellular carcinoma cell proliferation through up-regulation of cyclin D1," *Cellular Physiology and Biochemistry*, vol. 39, no. 2, pp. 700–708, 2016.

[31] T. Masaki, Y. Shiratori, W. Rengifo et al., "Hepatocellular carcinoma cell cycle: study of long-Evans cinnamon rats," *Hepatology*, vol. 32, no. 4, pp. 711–720, 2000.

[32] D. Santamaría, C. Barrière, A. Cerqueira et al., "Cdk1 is sufficient to drive the mammalian cell cycle," *Nature*, vol. 448, no. 7155, pp. 811–815, 2007.

[33] T. Toralová, A. Šušor, L. Němcová, K. Kepková, and J. Kaňka, "Silencing *CENPF* in bovine preimplantation embryo induces arrest at 8-cell stage," *Reproduction*, vol. 138, no. 5, pp. 783–791, 2009.

[34] C. L. Gao, G. W. Wang, G. Q. Yang, H. Yang, and L. Zhuang, "Karyopherin subunit-$\alpha$ 2 expression accelerates cell cycle progression by upregulating CCNB2 and CDK1 in hepatocellular carcinoma," *Oncology Letters*, vol. 15, no. 3, pp. 2815–2820, 2018.

[35] P. Jiang and D. Zhang, "Maternal embryonic leucine zipper kinase (MELK): a novel regulator in cell cycle control, embryonic development, and cancer," *International Journal of Molecular Sciences*, vol. 14, no. 11, pp. 21551–21560, 2013.

[36] H. Shuai, N. Li, Q. Zhang et al., "XAB2 functions in mitotic cell cycle progression via transcriptional regulation of CENPE," *Cell Death & Disease*, vol. 7, no. 10, article e2409, 2016.

[37] Y. Zhang, J. Liu, X. Peng et al., "KIF20A regulates porcine oocyte maturation and early embryo development," *PLoS One*, vol. 9, no. 7, article e102898, 2014.

[38] G. Hou, C. Dong, Z. Dong et al., "Upregulate KIF4A enhances proliferation, invasion of hepatocellular carcinoma and indicates poor prognosis across human cancer types," *Scientific Reports*, vol. 7, no. 1, p. 4148, 2017.

[39] A. K. Nandi and A. P. Rapoport, "Expression of PDZ-binding kinase (PBK) is regulated by cell cycle-specific transcription factors E2F and CREB/ATF," *Leukemia Research*, vol. 30, no. 4, pp. 437–447, 2006.

[40] W. Liao, W. Liu, Q. Yuan et al., "Silencing of DLGAP5 by siRNA significantly inhibits the proliferation and invasion of hepatocellular carcinoma cells," *PLoS One*, vol. 8, no. 12, article e80789, 2013.

[41] G. Liu, L. Wong, and H. N. Chua, "Complex discovery from weighted PPI networks," *Bioinformatics*, vol. 25, no. 15, pp. 1891–1897, 2009.

[42] J. Guo, X. Ma, Y. Cai et al., "Cytochrome P450 promiscuity leads to a bifurcating biosynthetic pathway for tanshinones," *New Phytologist*, vol. 210, no. 2, pp. 525–534, 2016.

[43] M. W. Yu, Y. H. Chiu, S. Y. Yang et al., "Cytochrome P450 1A1 genetic polymorphisms and risk of hepatocellular carcinoma among chronic hepatitis B carriers," *British Journal of Cancer*, vol. 80, no. 3-4, pp. 598–603, 1999.

[44] G. H. Hwang, S. M. Park, H. J. Han et al., "Role of cytochrome P450 2J2 on cell proliferation and resistance to an anticancer agent in hepatocellular carcinoma HepG2 cells," *Oncology Letters*, vol. 14, no. 5, pp. 5484–5490, 2017.

[45] J. Zhou, Q. Wen, S. F. Li et al., "Significant change of cytochrome P450s activities in patients with hepatocellular carcinoma," *Oncotarget*, vol. 7, no. 31, pp. 50612–50623, 2016.

[46] M. Ø. Pedersen, A. Larsen, M. Stoltenberg, and M. Penkowa, "The role of metallothionein in oncogenesis and cancer prognosis," *Progress in Histochemistry and Cytochemistry*, vol. 44, no. 1, pp. 29–64, 2010.

[47] M. Dabrio and A. R. Rodríguez, "Study of zinc metallothionein from rat liver using electrochemical techniques," *Electroanalysis*, vol. 12, no. 13, pp. 1026–1033, 2015.

[48] J. Datta, S. Majumder, H. Kutay et al., "Metallothionein expression is suppressed in primary human hepatocellular carcinomas and is mediated through inactivation of CCAAT/enhancer binding protein $\alpha$ by phosphatidylinositol 3-kinase signaling cascade," *Cancer Research*, vol. 67, no. 6, pp. 2736–2746, 2007.

[49] M. L. Mo, Z. Chen, J. Li et al., "Use of serum circulating CCNB2 in cancer surveillance," *International Journal of Biological Markers*, vol. 25, no. 4, pp. 236–242, 2010.

[50] X. Qian, X. Song, Y. He et al., "CCNB2 overexpression is a poor prognostic biomarker in Chinese NSCLC patients," *Biomedicine & Pharmacotherapy*, vol. 74, pp. 222–227, 2015.